ARTICLE

Jošt V. Lavrič · Jorge E. Spangenberg

Stable isotope (C, O, S) systematics of the mercury mineralization at Idrija, Slovenia: constraints on fluid source and alteration processes

Abstract The world-class Idrija mercury deposit (western Slovenia) is hosted by highly deformed Permocarboniferous to Middle Triassic sedimentary rocks within a complex tectonic structure at the transition between the External Dinarides and the Southern Alps. Concordant and discordant mineralization formed concomitant with Middle Triassic bimodal volcanism in an aborted rift. A multiple isotopic (C, O, S) investigation of host rocks and ore minerals was performed to put constraints on the source and composition of the fluid, and the hydrothermal alteration. The distributions of the $\delta^{13}C$ and $\delta^{18}O$ values of host and gangue carbonates are indicative of a fracture-controlled hydrothermal system, with locally high fluid-rock ratios. Quantitative modeling of the $\delta^{13}C$ and $\delta^{18}O$ covariation for host carbonates during temperature dependent fluid-rock interaction, and concomitant precipitation of void-filling dolomites points to a slightly acidic hydrothermal fluid ($\delta^{13}C \approx -4\permil$ and $\delta^{18}O \approx +10\permil$), which most likely evolved during isotopic exchange with carbonates under low fluid/rock ratios. The $\delta^{34}S$ values of hydrothermal and sedimentary sulfur minerals were used to re-evaluate the previously proposed magmatic and evaporitic sulfur sources for the mineralization, and to assess the importance of other possible sulfur sources such as the contemporaneous seawater sulfate, sedimentary pyrite, and organic sulfur compounds. The $\delta^{34}S$ values of the sulfides show a large variation at deposit down to hand-specimen scale. They range for cinnabar and pyrite from -19.1 to $+22.8\permil$, and from -22.4 to $+59.6\permil$, respectively, suggesting mixing of sulfur from different sources. The peak of $\delta^{34}S$ values of cinnabar and pyrite close to $0\permil$ is compatible with ore sulfur derived dominantly from a magmatic fluid and/or from hydrothermal leaching of basement rocks. The similar stratigraphic trends of the $\delta^{34}S$ values of both cinnabar and pyrite suggest a minor contribution of sedimentary sulfur (pyrite and organic sulfur) to the ore formation. Some of the positive $\delta^{34}S$ values are probably derived from thermochemical reduction of evaporitic and contemporaneous seawater sulfates.

J. V. Lavrič (✉) · J. E. Spangenberg
Institut de Minéralogie et Géochimie,
Université de Lausanne, BFSH2, 1015 Lausanne, Switzerland
E-mail: Jost.Lavric@img.unil.ch
Tel.: +41-21-6924449
Fax: +41-21-6924305

Introduction

The Idrija mercury ore field (46°00′10″N, 14°01′50″E) is located in the northwestern External Dinarides, about 50 km west of Ljubljana, Slovenia. The ore field includes mercury anomalies and economic concentrations in the Idrija and Ljubevč ore deposits (Fig. 1). The Idrija mine has been the second largest mercury mine in the world, having produced more than 12.7 Mt of ore with 145,000 t Hg since 1490 (Mlakar 1974), and is surpassed only by the Almadén mine (Spain) in the total metal quantity. Mining works in more than 150 orebodies extended vertically over more than 360 m (+330 to −33 m) on fifteen levels. The average ore grades decreased from the initial 17.0 wt% Hg to about 0.3 wt% Hg in recent times. The potential reserves of cinnabar and native mercury are estimated at 25,000 t Hg (Idrija Geological Department, personal communication). After 500 years of mining activity, the Idrija mine stopped production in 1988, and initiated a closing-down program, which is expected to finish in 2006. The Ljubevč ore deposit was discovered in 1962, but was never exploited commercially due to the relatively low ore grades (∼0.2 wt% Hg).

The geology and some genetic aspects of the Idrija deposit were described by Mlakar (1967), Mlakar and Drovenik (1971), Placer (1973, 1975, 1976, 1982),
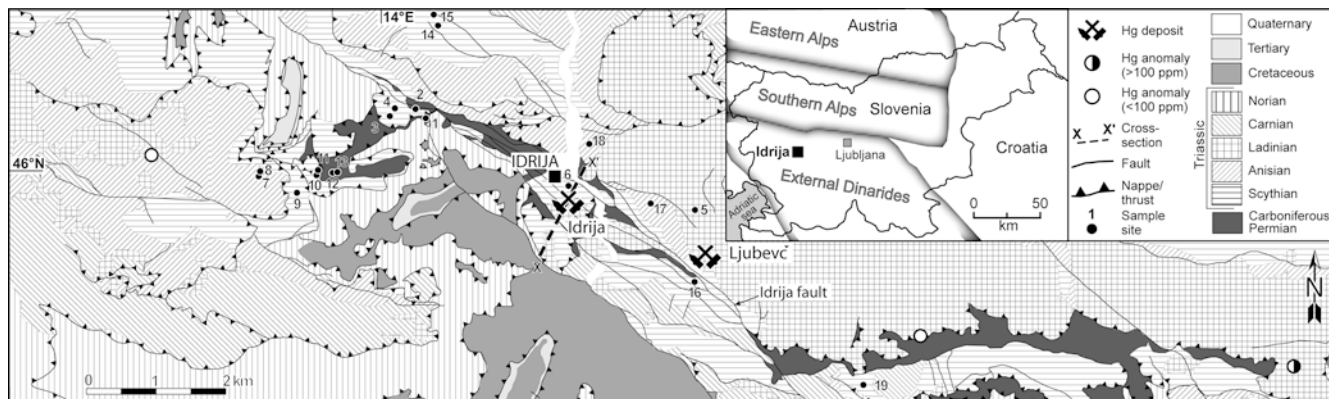
Fig. 1 Simplified geological map of the Idrija deposit area (modified after Mlakar 1969) and location of regional samples. Location of the Hg anomalies and cinnabar occurrences are from Placer and Čar (1977). See Fig. 3b for cross section

Drovenik et al. (1975), and Čar (1975, 1990). The geochemical investigations of the Idrija deposit include trace elements in cinnabar (Berce 1958; Drovenik et al. 1980), distribution of mercury at deposit scale (Berce 1965), trace element geochemistry of barren host rocks (Čadež et al. 1981), sulfur isotopes of sulfides and sulfates (Ozerova et al. 1973; Drovenik et al. 1976), a carbon, oxygen, and sulfur isotope study of an ore breccia at the Gruebler orebody (Drovenik et al. 1991), and mineralogical, molecular and isotopic characterization of the polycyclic aromatic hydrocarbon (PAH) mineral idrialite, found first associated to the Idrija ore (Strunz and Contag 1965; Blumer 1975; Wise et al. 1986; Spangenberg et al. 1999).

An ongoing extensive geochemical study of the Idrija deposit host rocks and the associated organic matter (e.g. Spangenberg et al. 1999; Lavrič and Spangenberg 2001, 2002), is aimed to contribute to a better understanding of the mineralization processes, and the relationship(s) of hydrothermal petroleum with the mercury ore. In this paper, we present new stable isotopic data of carbonates ($\delta^{13}C$, $\delta^{18}O$), sulfides ($\delta^{34}S$), and sulfates ($\delta^{34}S$, $\delta^{18}O$). These data serve to put constraints on the source and pathway of the ore fluid, the sulfur source, the extent of the hydrothermal alteration, and remobilization.
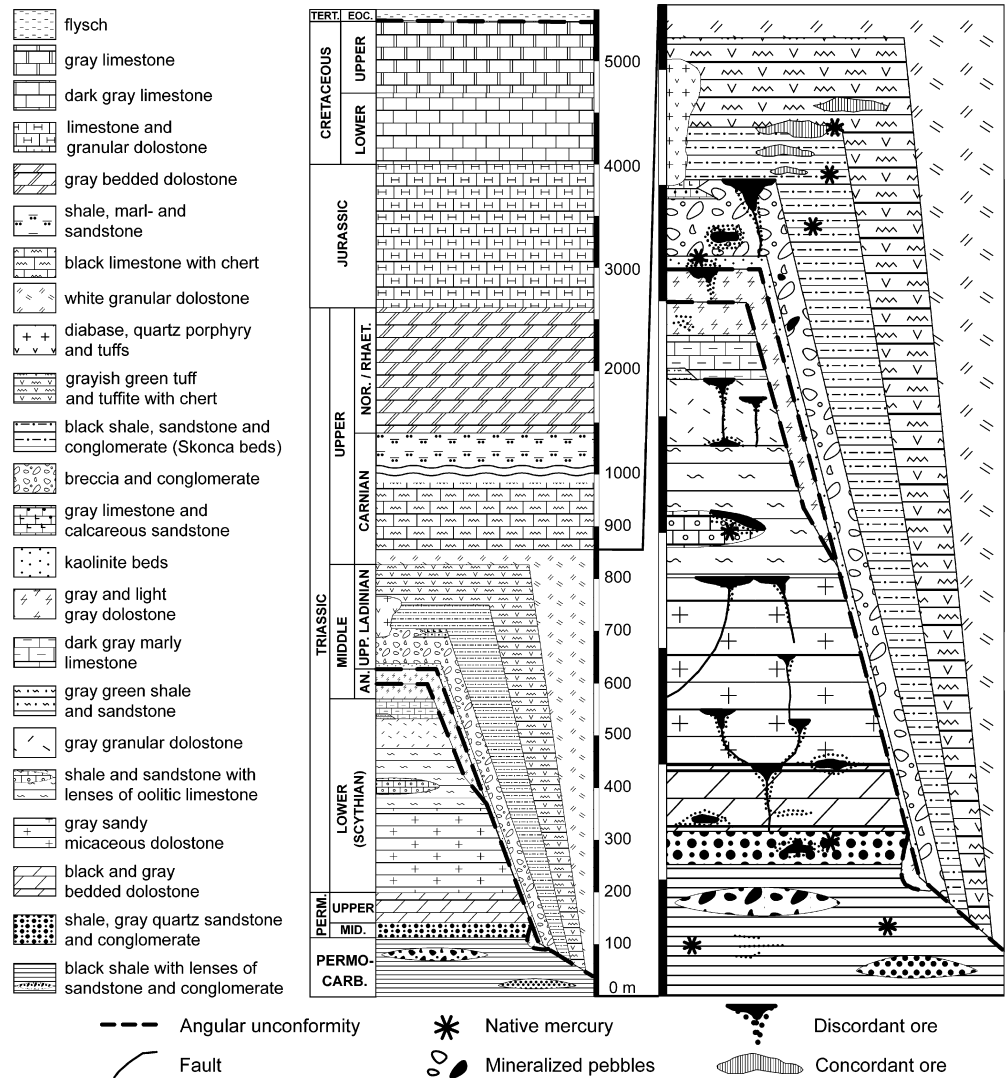
Geological setting

The Idrija mercury deposit is hosted by highly deformed sedimentary rocks of the Trnovo nappe, within a complex tectonic structure in western Slovenia. These sedimentary rocks were part of the Slovenian carbonate platform, which was cut into blocks by deep faults during E–W trending Middle Triassic intra-continental rifting (e.g. Placer and Čar 1977). The Ladinian rifting-induced effusive and explosive bimodal volcanism yielded volcanic products, which are found also at Idrija as grayish green tuff and tuffite, or as diabase (also as

pillow lavas), quartz porphyry and tuffs only some kilometers away. In the Late Triassic, the Julian and Dinaric carbonate platforms consolidated to the north and south of a deeper subsided Slovenian basin in the central part (Buser 1987). At Idrija, the estimated thickness of the Upper Triassic to Tertiary sedimentary cover was about 4,700 m (Fig. 2).

The Idrija structure was tectonically active from Early Scythian to Early Carnian. It developed in the apex of a dome in an approximately 1 km-wide and 5 km-long portion of an E–W trending failed rift (Idrija graben; Placer 1982). The rift was separated from sedimentary basins to the north and south by horsts (Fig. 3a; Placer and Čar 1977). It is not known whether the dome formed because of extension-related lithospheric uplift or due to emplacement of a laccolith (e.g. Placer 1982). Due to vertical displacement of up to 900 m along the N–S and E–W trending subvertical faults that formed at that time, the Idrija area was repeatedly exposed to subaerial processes, and locally covered by fresh water (e.g. Placer and Čar 1977). Two Middle Triassic regressive/transgressive cycles produced unconformities of a maximum range from Permocarboniferous to Upper Triassic (Fig. 2; Čar 1990). At the beginning of the second transgression, the part of the Idrija graben hosting the mineralization became an isolated basin with predominantly clastic sedimentation in a lacustrine and swamp environment (Čar 1985). The sedimentary rocks that formed were mainly shales, sandstones, and conglomerates. The beds overlying the second unconformity consist mainly of clasts of volcanic rocks, hydrothermally altered prior to their deposition (kaolinite beds in Fig. 2; Drovenik et al. 1975). The uppermost Ladinian sedimentary rocks (known by the local name of Skonca) were deposited in a shallow-water, highly vegetated environment under varying redox conditions (Čar 1985). The presence of radiolarians in the topmost part of this unit marks a gradual transition to a marine environment. At the Idrija mine area, the organic-rich Skonca beds were deposited coeval with enhanced tectonic and hydrothermal activity under acidic, reducing conditions (Čar 1985).

The Idrija host rocks were affected by two episodes of Alpine deformation (Placer 1982). The initial stage of

Fig. 2 Synthetic stratigraphic profile of the Idrija deposit showing types and locations of orebodies (modified after Čar 1990; Mlakar and Drovenik 1971)

Legend:

- flysch
- gray limestone
- dark gray limestone
- limestone and granular dolostone
- gray bedded dolostone
- shale, marl- and sandstone
- black limestone with chert
- white granular dolostone
- diabase, quartz porphyry and tuffs
- grayish green tuff and tuffite with chert
- black shale, sandstone and conglomerate (Skonca beds)
- breccia and conglomerate
- gray limestone and calcareous sandstone
- kaolinite beds
- gray and light gray dolostone
- dark gray marly limestone
- gray green shale and sandstone
- gray granular dolostone
- shale and sandstone with lenses of oolitic limestone
- gray sandy micaceous dolostone
- black and gray bedded dolostone
- shale, gray quartz sandstone and conglomerate
- black shale with lenses of sandstone and conglomerate

- - - Angular unconformity
- Fault
- Native mercury
- Mineralized pebbles
- Discordant ore
- Concordant ore

the Early Tertiary phase resulted in the formation of a synclinal fold with its axis oblique (112°N) to that of the E–W trending Idrija graben. Later, regional-scale NNE–SSW thrusting overturned the fold, cut the deposit horizontally into three units, and displaced them approximately 30 km toward SSW. During thrusting, the lowermost unit (the former southern part of the mineralized Idrija graben) stayed behind, and is today presumably located somewhere to the NNE of Idrija (Placer 1982). A Late Tertiary tectonic phase cut the deposit with dextral NW–SE strike-slip faults into blocks, and displaced them sub-horizontally up to 2 km (Fig. 3b). At that time, a part of the deposit was divided along the Idrija fault into the Idrija and Ljubevč deposits (Fig. 1), while other parts were uplifted and eroded (Placer 1982).

The Idrija deposit

The stratigraphic succession at the Idrija deposit comprises about 5,500 m of sedimentary and volcanic rocks of Permocarboniferous to Eocene age, of which the lowermost 800 m host the mineralization (Fig. 2). The host rocks are strongly disturbed by folding and thrusting. A detailed petrographical and mineralogical description of the Idrija mineralization is given by Mlakar and Drovenik (1971), and is briefly summarized here. The ore zones include concordant and discordant mineralization. Concordant orebodies formed during sedimentation of the Upper Ladinian organic-rich Skonca beds (~1.4 wt% TOC; Lavrič and Spangenberg, unpublished data) and the overlying tuff. They are stratiform or lens-shaped, up to 100 m long and 0.5 m thick, and show synsedimentary structures. The ore grade (up to 79 wt% Hg) and number of orebodies increase stratigraphically upwards. Several generations of discordant veinlets in the concordant orebodies are attributed to post-mineralization deformation and remobilization of ore and gangue minerals. The discordant mineralization is associated to fault zones in Permocarboniferous to Upper Ladinian beds. It occurs as veins and open-space fillings, replacement in carbonate rocks, and replacement of carbonate cement in

Fig. 3 Schematic section of the Idrija deposit **a** at the time of ore deposition in Middle Triassic and **b** at present time (modified after Mlakar 1967; Placer and Čar 1977; Čar 1990). *Numbers* denote major Middle Triassic faults: *1* Zagoda, *2* Veharše, *3* Talnina, *4* Močnik, *5* Čemernik, *6* Karoli, *7* Gruebler, *8* Bačnar, *9* Urbanovec-Zovčan, *10* Gugler, *11* Auersperg, *12* Kropač, *13* Zilja, *14* Pront, *15* Zajele. See Fig. 1 for location of cross section (X–X') and Fig. 2 for legend of lithological units
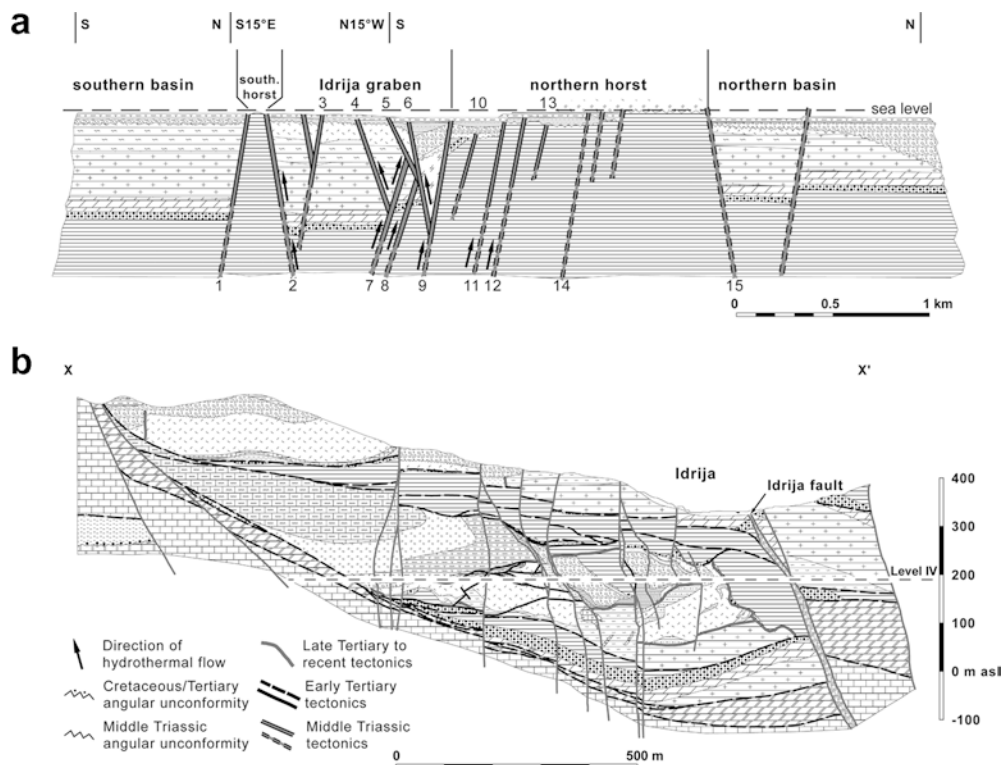
clastic rocks. The orebodies extend vertically often more than 100 m. Their upper flat parts are controlled by less permeable lithostratigraphic units or the Middle Triassic unconformities, and can be up to some tens of meters wide and over 100 m long. Exceptional is the Karoli orebody, because it is the only orebody that formed in association with a network of fractures close to a major feeder zone (Urbanovec-Zovčan and Karoli faults; Fig. 3a) in a Ladinian olisthostrome (Placer and Čar 1977). This orebody is interpreted as having formed by hydrothermal impregnation of the unlithified sediments (Čar 1985). In the Gruebler orebody, the discordant mineralization formed at the tectonic contact of Lower Scythian dolostone and Permocarboniferous black shale, at a depth of approximately 750 m (Placer 1975). A study of mono-, two-, and multiphase inclusions in euhedral quartz and barite crystals, and irregular cinnabar crystals from this orebody (Palinkaš et al. 2001), points to moderately hot (T_h = 160 to 218 °C), and low to moderately saline (2.6 to 12.8 eq wt% NaCl) H_2O–NaCl–$CaCl_2$ fluids. The homogenization temperature could not be measured in cinnabar and barite due to decrepitation, but the salinity (3.6 to 9.1 eq wt% NaCl) and NaCl/$CaCl_2$ ratios (0.57 to 1.60) are similar to those measured in quartz (2.6 to 12.8 eq wt% NaCl and 0.63 to 1.53). The barite and quartz crystals contain numerous cinnabar inclusions, suggesting that they may be coeval with the mercury mineralization. The chemical composition of the trapped fluids is similar to that of hydrothermal fluids generated during extrusion of pillow lavas during Triassic rifting within the Zagorje–Mid-Transdanubian zone, NW Croatia (Palinkaš et al. 2001).

Mlakar and Drovenik (1971) proposed that Idrija formed during the Scythian-Ladinian aborted rifting and bimodal volcanism by venting of near neutral mercuriferous hydrothermal fluids at the seafloor. Idrija is therefore regarded as a sedimentary-exhalative (SEDEX) deposit. A system of deep, N–S and E–W orientated subvertical faults (e.g. Urbanovec-Zovčan, Čemernik, and Karoli faults; Fig. 3a) within the Idrija graben focused the flow of the mineralizing fluids. The Idrija mineralization is characterized by two major phases (Mlakar and Drovenik 1971). Phase I cinnabar occurs as replacement and open-space fillings in Permocarboniferous to Anisian rocks. It predates the second erosion phase, as evidenced by mineralized plagioclase and tuff fragments embedded in the non-mineralized matrix of the kaolinite beds, and pebbles of mineralized Upper Scythian dolostone in the Upper Ladinian conglomerate overlying the kaolinite beds (Fig. 2). Phase II coincided with the deposition of the Upper Ladinian Skonca beds and the overlying volcaniclastic rocks. During this phase, the hydrothermal solutions further mineralized the Permocarboniferous to Anisian rocks, mineralized the Upper Ladinian conglomerates, and emanated at the seafloor as thermal springs producing concordant orebodies (Fig. 2).

Ore and gangue minerals

The generalized paragenetic sequence (Fig. 4) was compiled from the findings of Mlakar and Drovenik (1971), Drovenik et al. (1991), and our own

Early ——————————————→ Late

Stage / Mineral	Pre-ore	Ore Phase I	Ore Phase II	Post-ore
Cinnabar		– – – – ?	▬▬▬▬	– – – –
Metacinnabar		– – – ? – ·	– – – – –	
Native mercury		– – – ? – ·	▬▬▬	– – ? –
Pyrite/Marcasite (sed.)	▬▬ – – – –			
Pyrite (hyd.)		– – – ? – ·	▬▬▬	
Quartz		– – – ? – ·	▬▬▬	– – – –
Chalcedony			▬▬▬	
VFC		– – – – –	– – – – –	– – – –
VFD		▬▬▬▬		– – – –
Gypsum/Anhydrite	▬▬▬			
Barite			– – – –	
Fluorite				– –
Hydrocarbons	– – –	▬▬▬▬	▬▬▬▬	– – – – –

Fig. 4 The mineral assemblage and paragenetic sequence of the Idrija deposit (compiled and modified after Mlakar and Drovenik 1971; Drovenik et al. 1991). *Thick*, *thin*, and *dashed bars* represent major, minor and rare occurrence of minerals in individual stages, respectively. *Sed.* sedimentary, *hyd.* hydrothermal, *VFC* void-filling calcite, *VFD* void-filling dolomite. Hydrocarbons include free hydrocarbons, idrialite and pyrobitumen

observations. The ore consists of cinnabar and native mercury, with minor pyrite and metacinnabar. Sedimentary pyrite and marcasite are present in all mineralized lithologies, most notably as concretions in the Permocarboniferous black shale, and disseminated in the Upper Permian dolostone and the Upper Ladinian sedimentary rocks. Native mercury accounts for ~10% of the cumulative production (Mlakar 1996). Very high pyrite contents (50 to 90 wt%) are found locally in the Karoli orebody. Based on different textures (pebbles, concretions, anhedral to euhedral metacrystals, veinlets), previous investigators tentatively interpreted this pyrite to be of both hydrothermal and sedimentary origin, partly as an erosion product of the Permocarboniferous and the Ladinian rocks (Mlakar and Drovenik 1971; Čar 1985). Hydrothermal pyrite occurs also in Triassic fault zones associated to pyrobitumen. The main gangue minerals are quartz, calcite, and dolomite, with very rare barite and fluorite. The stratiform ore contains chalcedony and siliceous microfossils, such as radiolarians and sponge spicules (Mlakar and Drovenik 1971). Evaporitic gypsum and anhydrite occur in up to 1.5 m-thick lenses in the Upper Permian and Lower Scythian dolostones (Čadež 1977). Different generations of carbonates can be distinguished. They include host-rock carbonates (dolomite and calcite), and void-filling dolomite (VFD) or calcite (VFC). The host-rock carbonates are fine- to medium-crystalline dark dolomite or calcite, with total organic carbon (TOC) content of up to 0.53 wt% (Lavrič and Spangenberg, unpublished data). The void-filling carbonates are medium- or coarse-grained, mainly anhedral, milky-white dolomite (VFD) or calcite (VFC).

A part of cinnabar occurs as open-space filling, together with the carbonates. Weak silicification is observed in the mineralized Middle Triassic fault zones.

Pyrobitumen (slightly soluble in organic solvents) occurs as open-space filling in discordant mineralization. Amorphous organic matter is interbedded with the Skonca ore. Aromatic hydrothermal petroleum and solid aromatic hydrocarbons (idrialite) also occur associated to the Idrija ore (Spangenberg et al. 1999).

Sampling and analytical methods

Sampling

The host rocks were sampled at a regional and mine scale. Nineteen regionally distributed barren samples, comprising the complete host-rock sequence, were taken at outcrops not farther than 6 km from the deposit (Fig. 1). Extensive multiple sampling was made at the Idrija mine, including orebody, outcrop and hand-specimen scale. A total of 125 samples of the Permocarboniferous to Upper Ladinian mineralized lithologies were taken from mine walls at different levels. The remains of the intensively mined Karoli orebody were accessible only on one outcrop on level IV, where three samples were taken. The isotopic zonation and possible pathway of the mineralizing fluid were investigated in profiles extending from highly mineralized into barren zones. Samples (n=111) of Upper Permian to Upper Ladinian rocks were collected in 7 profiles at level IV (157 m below surface), with a total length of 725 m, and sampling intervals between 5 and 10 m. The short-scale geochemical zonation was studied at two mine walls of about 3×2.5 m^2 in highly mineralized Lower Scythian siltstone and dolostone, and in hand-specimens of mineralized Upper Ladinian conglomerate and Karoli ore. Additional 41 ore samples from exhausted orebodies and inaccessible (backfilled or flooded) areas of the mine were obtained from collections of the Idrija mine, the Department of Geology of the Ljubljana University, and the Cantonal Geological Museum of Lausanne.

Analytical methods

The carbonates and sulfur minerals were sampled from fresh surfaces of the hand-specimens using a diamond drill. Carbon and oxygen isotope analyses were done for all host carbonate samples (19 regional, 71 mine), and 36 void-filling dolomite (VFD) and calcite (VFC) samples. The mineralogical composition of the host and void-filling carbonates was determined with acid test (HCl), and X-ray diffraction when necessary. Extraction of CO_2 from the carbonates was done by reaction with 100% phosphoric acid (4 h, 50 °C) in a closed reaction vessel (McCrea 1950). Carbon and oxygen isotopic compositions were measured via dual inlet on a Thermoquest/Finnigan Delta S mass spectrometer. The results were corrected for carbonate–phosphoric acid fractionation using the factors of 1.010600 for dolomite (Rosenbaum and Sheppard 1986), and 1.009311 for calcite (Friedman and O'Neil 1977). The $\delta^{13}C$ and $\delta^{18}O$ values are reported as per mil (‰) relative to the V-PDB and V-SMOW standards, respectively. Analytical uncertainty, assessed by replicate analyses of the laboratory standard (Carrara marble, $\delta^{13}C = +2.1$‰ and $\delta^{18}O = +29.4$‰), is less than ± 0.05‰ for $\delta^{13}C$ and ± 0.1‰ for $\delta^{18}O$ (1 SD).

Two hundred fifty-seven sulfides (cinnabar, pyrite) and four sulfates (gypsum, barite) have had their sulfur isotopic composition determined. The sulfur isotope analyses were done using a Carlo Erba 1108 elemental analyzer—continuous flow—isotope ratio Thermoquest/Finnigan Delta S mass spectrometer (EA/IRMS) system (Giesemann et al. 1994). The sulfur isotope values are reported as per mil relative to the V-CDT standard. The reproducibility of the EA/IRMS measurements, evaluated by replicate

analyses of laboratory standards (barium sulfate, $+12.5\permil$; pyrite, $-7.0\permil$; synthetic cinnabar, $+15.5\permil$) is better than $\pm 0.2\permil$ (1 SD). The oxygen isotopic composition of barite from the Gruebler orebody was measured with a high temperature conversion elemental analyzer (TC/EA) coupled to a Thermoquest/Finnigan Delta Plus XL isotope ratio mass spectrometer. The reproducibility of the TC/

EA/IRMS measurements, assessed by replicate analyses of the laboratory standard (barium sulfate, $\delta^{18}O = +14.0\permil$), is better than $\pm 0.3\permil$ (1 SD).

Results

Carbonates

Carbon and oxygen isotope data are presented in Fig. 5 and summarized in Table 1. The $\delta^{13}C$ and $\delta^{18}O$ values for regional and mine host-rock carbonates range from -2.2 to $+5.6\permil$ and $+22.0$ to $+30.1\permil$, respectively, for VFD from $+0.6$ to $+5.0\permil$ and $+19.4$ to $+26.4\permil$, and for VFC from -0.3 to $+0.3\permil$ and $+19.7$ to $+23.7\permil$. Overall, the carbonates have a marine isotopic signature, and exhibit approximately positive $\delta^{13}C$ vs. $\delta^{18}O$ covariation (Fig. 5). The isotopically heaviest carbonates are the regional Upper Permian dolostone (Table 1). Regional host carbonates generally have a similar isotopic composition as the barren or slightly mineralized host carbonates from the Idrija mine (Fig. 5). A trend toward lighter oxygen isotopic composition is observed in the following sequence: regional host carbonates → mine host carbonates → VFD → VFC. For the Upper Permian, Lower Scythian and
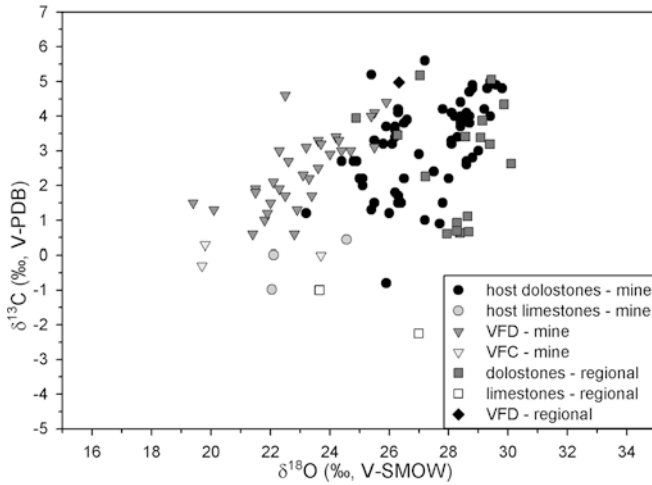

Fig. 5 $\delta^{13}C$ vs. $\delta^{18}O$ plot of carbonates from the Idrija mine and barren regional outcrops

Table 1 Carbon and oxygen isotope composition of host carbonates and void-filling carbonates from the Idrija mine and regional barren outcrops

Lithological unit (n)[a] Field code[b]		$\delta^{13}C$ (‰, V-PDB)		$\delta^{18}O$ (‰, V-SMOW)	
		Range	Median	Range	Median
Upper Ladinian limestone					
Regional (1)	5	-2.2	-2.2	$+27.0$	$+27.0$
Mine (1)		$+0.4$	$+0.4$	$+24.5$	$+24.5$
VFC, mine (1)		0.0	0.0	$+23.7$	$+23.7$
Upper Ladinian conglomerate					
VFD, mine (4)		$+0.6$ to $+1.5$	$+1.3$	$+21.4$ to $+22.9$	$+22.0$
Anisian dolostone					
Regional (4)	7, 8, 17, 18	$+2.3$ to $+3.4$	$+3.3$	$+27.2$ to $+29.4$	$+28.7$
Mine (6)		$+2.2$ to $+3.0$	$+2.7$	$+27.5$ to $+29.0$	$+28.6$
VFD, mine (1)		$+0.6$	$+0.6$	$+22.8$	$+22.8$
Upper Scythian dolostone					
Regional (4)	3, 14, 15, 19	$+0.6$ to $+2.6$	$+0.8$	$+28.2$ to $+30.1$	$+28.3$
Mine (4)		$+0.9$ to $+5.6$	$+1.3$	$+27.2$ to $+27.8$	$+27.4$
Lower Scythian shale					
VFD, mine (3)		$+1.3$ to $+4.6$	$+1.5$	$+19.4$ to $+22.5$	$+20.1$
Lower Scythian oolitic limestone					
Regional (1)	2	-1.0	-1.0	$+23.7$	$+23.7$
Mine (2)		-1.0 to 0.0	-0.5	$+22.0$ to $+22.1$	$+22.1$
VFC, mine (2)		-0.3 to $+0.3$	0.0	$+19.7$ to $+19.8$	$+19.8$
Lower Scythian dolostone					
Regional (6)	4, 6, 9, 10, 11, 16	$+0.6$ to $+3.9$	$+2.3$	$+24.9$ to $+29.2$	$+28.3$
Mine (18)		-0.8 to $+5.2$	$+2.1$	$+24.8$ to $+26.5$	$+25.7$
VFD, mine (6)		$+1.0$ to $+2.1$	$+1.9$	$+21.5$ to $+22.5$	$+21.9$
Upper Permian dolostone (UPD)					
Regional (3)	1, 12, 13	$+4.3$ to $+5.2$	$+5.1$	$+27.0$ to $+29.9$	$+29.5$
Mine (40)		$+1.2$ to $+5.0$	$+4.0$	$+23.2$ to $+29.8$	$+28.4$
VFD, regional (1)		$+5.0$	$+5.0$	$+26.4$	$+26.4$
VFD, mine (18)		$+1.7$ to $+4.4$	$+3.1$	$+22.3$ to $+25.9$	$+23.8$

[a] *VFD* Void-filling dolomite, *VFC* void-filling calcite, *n* number of analyzed samples
[b] Numbers correspond to sampling sites of regional samples shown in Fig. 1

Anisian dolostones the same, but less pronounced trend is observed also for carbon (Fig. 5).

Sulfides and sulfates

The ranges and the median sulfur isotope compositions of the analyzed sulfide and sulfate minerals are summarized in Table 2, and are graphically presented in Figs. 6 and 7. The $\delta^{34}S$ values for all cinnabar samples ($n=166$) range from -19.1 to $+22.8‰$, with a peak at $\sim+2‰$ (Fig. 6a). At orebody scale, the values cover a range of $\sim20‰$, whereas the small-scale variation in the studied mine walls is $\sim9‰$ (-2.8 to $+1.2‰$ in Lower Scythian dolostone, and -3.6 to $+5.8‰$ in Lower Scythian shale). In concordant orebodies, the massive cinnabar and the late, fissure-filling cinnabar have median $\delta^{34}S$ values of $+0.8‰$ ($n=7$) and $+14.7‰$ ($n=6$), respectively. The $\delta^{34}S$ values of all pyrite samples ($n=91$) range from -22.4 to $+59.6‰$, having a median value of $-0.2‰$ (Fig. 6b). The most prominent peak in the distribution of the pyrite $\delta^{34}S$ values is at $\sim0‰$ (Fig. 6b). The hydrothermal euhedral pyrite (up to 1 cm-sized crystals) in Middle Triassic fault zones ($n=15$) has $\delta^{34}S$ values ranging from -3.2 to $+0.4‰$, with a median value of $-0.7‰$. On a deposit scale, the $\delta^{34}S$ values for cinnabar and pyrite increase stratigraphically upward, with a negative excursion in the Upper Permian dolostone, and the heaviest values in the Upper Ladinian (Fig. 7a, b).

The cinnabar from the Karoli ore hand-specimen ($n=11$) has $\delta^{34}S$ values in the narrow range of $+0.1$ to $+1.4‰$, and a median value of $+0.6‰$ (Fig. 8). The pyrite ($n=20$) has $\delta^{34}S$ values in the range of -2.0 to $+6.5‰$, with a median isotopic composition of $-1.3‰$ (Fig. 8). These values are similar to those of pyrite from fault zones (median $=-0.7‰$). The $\delta^{34}S$ values of both pyrite and cinnabar from this hand-specimen are comparable to those in the other two Karoli ore hand-specimens. In the Upper Ladinian conglomerate hand-specimen the cinnabar associated to the void-filling dolomite is isotopically heavier ($+6.0$ to $+11.5‰$, median $=+8.2‰$, $n=6$) than the cinnabar replacing the conglomerate matrix ($+2.6$ to $+8.9‰$, median $=+4.2‰$, $n=7$). The $\delta^{34}S$ values of pyrite ($n=16$) have a wide range of -2.0 to $+59.6‰$.

The gypsum samples ($+12.3$ and $+16.4‰$) are within the range of Permian to Middle Triassic marine evaporites (Claypool et al. 1980). The oxygen and sulfur isotopic ratios of barite crystals from the Gruebler orebody are $+19.5$ and $+20.4‰$ V-SMOW, and $+46.6$ and $+52.3‰$ V-CDT, respectively.

Discussion

The Idrija hydrothermal system is accepted to have been active during most of the Ladinian (e.g. Čar 1990).

Table 2 Sulfur isotope data of sulfides and sulfates from the Idrija mine

Age of host rock	Min.[a]	n[b]	$\delta^{34}S$ (‰, V-CDT)	
			Range	Median
Upper Ladinian	ci	40	-3.6 to $+22.8$	$+6.7$
	py	11	-2.0 to $+0.7$	-0.7
	py(s)	31	-7.8 to $+59.6$	$+17.7$
Ladinian (Karoli)[c]	ci	14	$+0.1$ to $+3.2$	$+0.8$
	py	24	-2.0 to $+6.5$	-1.2
Anisian	ci	10	$+3.1$ to $+8.0$	$+4.9$
Upper Scythian	ci	3	$+4.9$ to $+7.0$	$+5.6$
	py	1	$+6.6$	$+6.6$
Lower Scythian	ci	39	-3.6 to $+5.8$	$+0.6$
	py	10	-3.2 to $+13.2$	$+4.8$
	bar	2	$+46.6$ to $+52.3$	$+49.5$
Upper Permian	ci	34	-19.1 to $+7.7$	-6.4
	gy	2	$+12.3$ to $+16.4$	$+14.3$
	py	4	-1.6 to 0.0	-0.6
	py(s)	3	-22.4 to -15.6	-17.5
Middle Permian	ci	3	$+0.1$ to $+6.2$	$+2.6$
	py	4	-1.0 to -0.1	-0.4
Permocarboniferous	ci	1	-4.9	-4.9
	py(s)	3	-0.2 to $+4.8$	$+3.0$

[a]Minerals analyzed: *bar* barite, *ci* cinnabar, *gy* gypsum, *py* pyrite, *py(s)* sedimentary pyrite
[b]Number of analyzed samples. Cinnabar samples from collections with unknown stratigraphic position ($n=22$) are not included
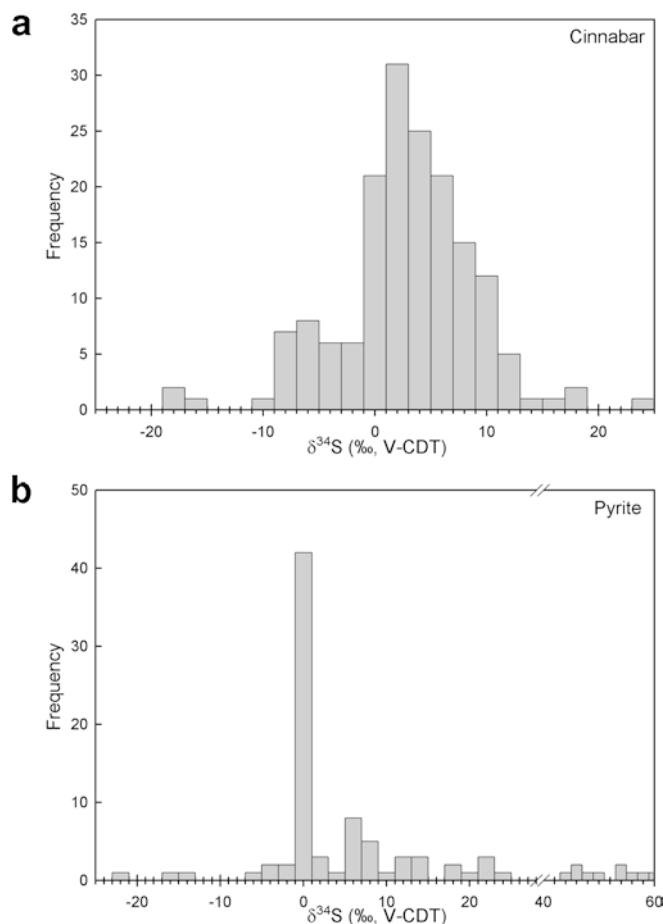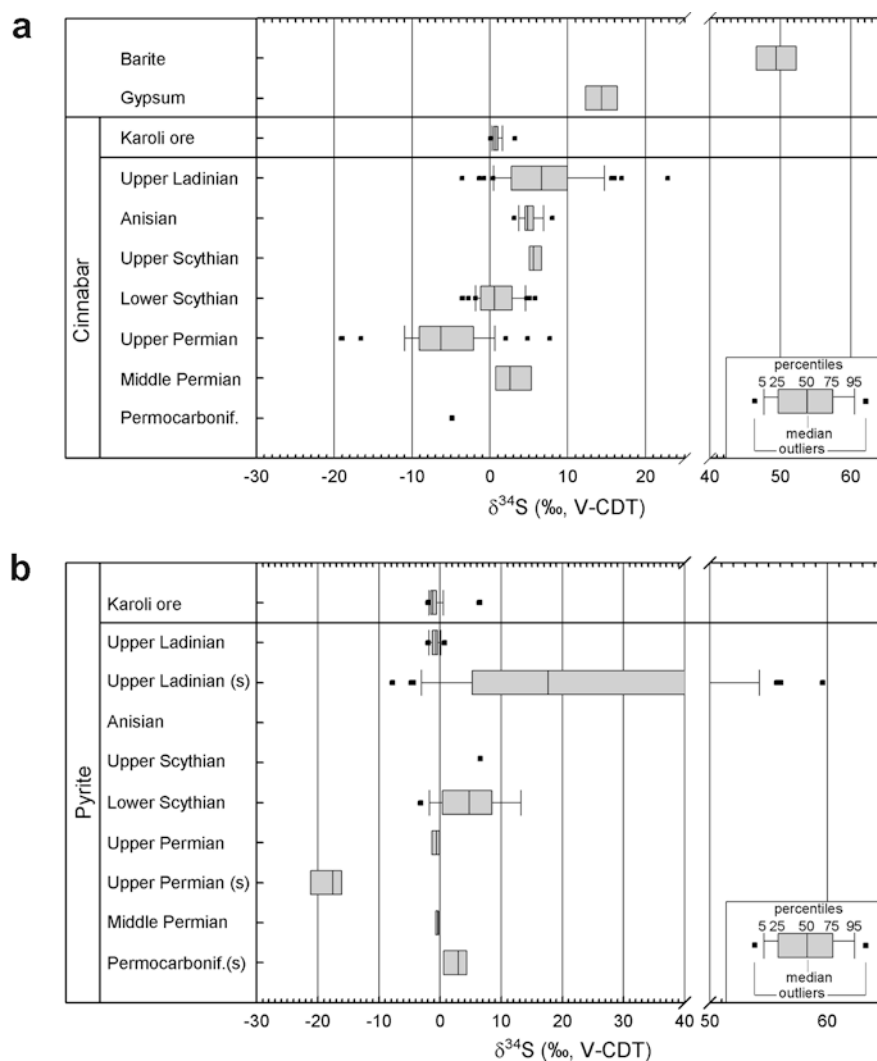[c]Karoli orebody

Fig. 6 Frequency distribution of $\delta^{34}S$ values for **a** cinnabar and **b** pyrite

Fig. 7 Ranges and medians of δ^{34}S values of all analyzed samples of **a** cinnabar and sulfates, and **b** pyrite. *s* denotes sedimentary pyrite. All outliers are shown. See Table 2 for number of samples

Therefore, it may be expected that long-term physico-chemical changes induced variations in the chemical and isotopic composition of the mineralizing fluids. The stable isotope compositions of ore and gangue minerals may record these changes, providing information on the temperature, composition, source, and pathway of the fluids.

Temperature of mineralization

The temperatures of mercury mineralization at shallow depth in most recent and fossil hydrothermal systems are believed to be below 250 °C (e.g. Varekamp and Buseck 1984; Peabody and Einaudi 1992). For example, the temperature was below 160 °C in the New Idria district (Boctor et al. 1987), between 135 and 240 °C in the Mayacmas district (Peabody and Einaudi 1992), and below 150 °C in the active hydrothermal system at Sulphur Bank (White 1981).

Fluid inclusion data for cinnabar, quartz and barite from the Gruebler orebody indicate mineralization

temperatures between 160 and 218 °C at a depth of ~750 m (Palinkaš et al. 2001). At Idrija, coexisting pyrite and cinnabar have an isotopic fractionation ($\Delta^{34}S_{FeS2-HgS}$) of less than +3‰. Application of the equilibrium fractionation factors of Ohmoto and Goldhaber (1997) gives unrealistically high temperatures (>330 °C), suggesting lack of equilibrium between these sulfides. Barite from the Gruebler orebody is isotopically heavier ($\delta^{18}O \approx +20\%$, $\delta^{34}S \approx +49\%$) than the Permian to Tertiary seawater sulfates ($\delta^{18}O \approx +7$ to +12‰, $\delta^{34}S \approx +10$ to +22‰; Claypool et al. 1980) or barite from active hydrothermal vents (e.g. $\delta^{18}O \approx +7\%$, $\delta^{34}S \approx +22\%$ for barite from Mariana Trough; Kusakabe et al. 1990). ^{34}S- and ^{18}O-enriched barite has been reported in different geological settings, including the hydrothermal system at Creede (Rye et al. 1988), the convergent margin off Peru (Aquilina et al. 1997), and the barite concretions in the West Carpathian flysch, Poland (Leśniak et al. 1999). Such coupled sulfur and oxygen isotopic enrichment of barite is interpreted to arise from crystallization of isotopically heavy residual sulfate, which went through cycles of bacterial sulfate
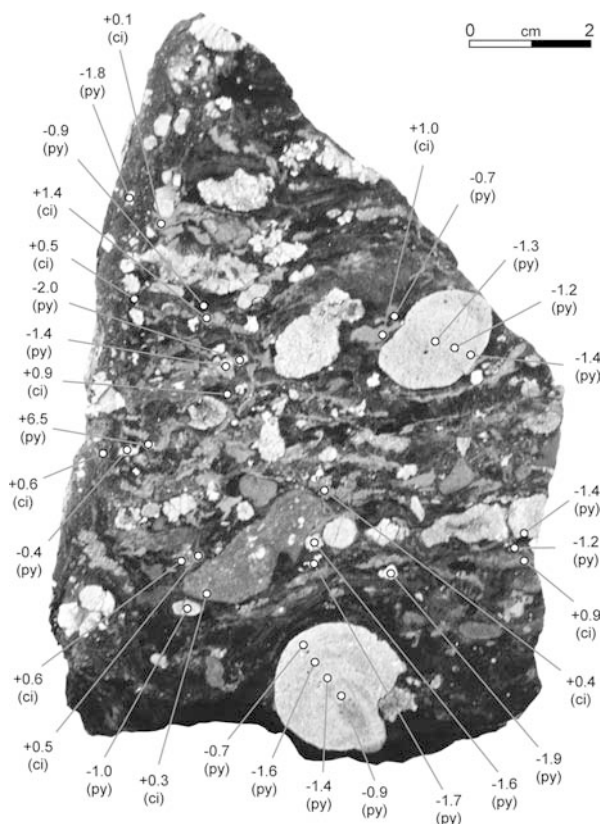
+0.1
(ci)
-1.8
(py)
-0.9
(py)
+1.4
(ci)
+0.5
(ci)
-2.0
(py)
-1.4
(py)
+0.9
(ci)
+6.5
(py)
+0.6
(ci)
-0.4
(py)
+0.6
(ci)
+0.5
(ci)
-1.0
(py)
+0.3
(ci)
-0.7
(py)
-1.6
(py)
-1.4
(py)
-0.9
(py)
-1.7
(py)
-1.6
(py)
-1.9
(py)
+0.4
(ci)
+0.9
(ci)
-1.2
(py)
-1.4
(py)
-1.4
(py)
-1.2
(py)
-1.3
(py)
-0.7
(py)
+1.0
(ci)

0 cm 2

Fig. 8 Sulfur isotope composition of cinnabar and pyrite in a hand-specimen of the Karoli ore (*ci* cinnabar, *py* pyrite)

reduction (BSR), combined with re-equilibration of sulfate oxygen with water oxygen at elevated temperatures (e.g. Leśniak et al. 1999). It is, however, not necessary to invoke BSR to explain the enrichment in ^{34}S, as isotopically heavy sulfur will concentrate in the sulfate ion in any highly H_2S-dominated system, independently of the type of the reduction process. Oxygen isotopic equilibrium between seawater and sulfate at neutral pH is unlikely at low temperatures (e.g. Chiba and Sakai 1985). Therefore, the $\delta^{34}S$ and $\delta^{18}O$ values together with the fluid inclusion data suggest, that the barite from the Gruebler orebody precipitated from moderately hot (160 to 220 °C) hydrothermal fluids, and not from percolating groundwater, in a low-temperature environment during the Alpine uplift, as proposed by Drovenik et al. (1991).

Sulfur source

The sulfur isotope composition of the sedimentary and hydrothermal sulfides was used to determine the source of sulfur in the mineralizing fluid(s). The wide ranges of $\delta^{34}S$ values of cinnabar ($>40‰$) and pyrite ($>80‰$) are compatible with sulfur sources of variable isotopic composition and/or changes of the physicochemical conditions during their formation. The abundance of hydrothermal sulfides and very rare occurrence of hydrothermal sulfates point to a reducing and H_2S-rich environment during ore formation. Previous investigators have suggested that the reduced sulfur in the Idrija hydrothermal system was of a magmatic (Drovenik et al. 1976) or evaporitic (Ozerova et al. 1973) origin. Middle Triassic seawater sulfate, sedimentary pyrite and organic sulfur are further possible sulfur sources to be considered.

The distribution of the $\delta^{34}S$ values of the Idrija ore sulfides from the Lower Scythian to Upper Ladinian beds (Fig. 7) notably resembles to that of massive sulfides from modern seafloor ridges (e.g. Herzig et al. 1998 and references therein). The reduced sulfur in such systems is a mixture of magmatic sulfur and sulfur derived from thermochemical sulfate reduction (TSR). Consequently, the $\delta^{34}S$ values of the sulfides lie somewhere between the isotopic compositions of the two end members, depending on the relative contributions of these sources.

The $\delta^{34}S$ values of the sulfides close to 0‰ for the Middle Triassic fault zones, Karoli ore, and the concordant Skonca ore are most readily explained by a magmatic sulfur source. Additionally, given the association of the mineralization with the Triassic volcanism (Mlakar and Drovenik 1971), and the formation of the ore at sites of high permeability, it is conceivable that a part of the ore sulfur was derived from a magmatic fluid or from hydrothermal leaching of basement rocks. The $\delta^{34}S$ values of the Karoli ore sulfides suggest that the Permocarboniferous and the Ladinian rocks were not the source of pyrite in this orebody. What were termed pyrite "pebbles" by previous investigators (e.g. Čar 1985) may actually be diagenetic concretions, which were possibly transported on short distances during the formation of the Ladinian olisthostrome in a reducing environment. This assumption is supported also by pebble-like pyrite concretions found in samples from this study (Fig. 8).

The source of positive $\delta^{34}S$ values in the hydrothermal sulfides could be sulfur derived from TSR of Permotriassic evaporites and contemporaneous seawater at elevated temperatures (>90 °C; Krouse et al. 1988), with local hydrocarbons as the electron donor. This may be supported by the high concentration of aromatic hydrocarbons and other oxidized organic compounds in the bitumen extracted from ore samples or intergrown with cinnabar (Spangenberg et al. 1999; Lavrič and Spangenberg 2002). The few $\delta^{34}S$ values of pyrite from Karoli ore that deviate significantly from the median value of $-1.3‰$ ($+6.4$ and $+6.5‰$) belong to paragenetically late hydrothermal pyrite. They may be interpreted as the product of mixing of distinct sulfur sources in an advanced stage of the mineralization process, due to a larger input of isotopically heavier, sulfate-derived sulfur. This would be in line with the advancing transgression during the Ladinian.

An additional source of sulfur can be leaching of diagenetic sulfides or organic sulfur compounds from

the enclosing host rocks. The most likely sources of sedimentary sulfur are the Permocarboniferous black shale and the Upper Permian dolostone, which host sedimentary pyrite with $\delta^{34}S$ in the range of -22.4 to $+4.8‰$, and contain significant amounts of organic sulfur compounds also in barren areas (Lavrič and Spangenberg 2002). Although the $\delta^{34}S$ values of organic sulfur compounds were not measured, it is generally accepted that their values are similar to, or higher than those of the co-existing sedimentary pyrite (e.g. Ohmoto and Goldhaber 1997). The negative excursion of the $\delta^{34}S$ values of cinnabar in the Upper Permian and the overlying Lower Scythian dolostones (Fig. 7a) suggests a contribution of isotopically light sulfur from bacteriogenic sulfides and organic sulfur compounds to the hydrothermal fluids. This is also supported by the replacement of diagenetic pyrite concretions with cinnabar observed in the Permocarboniferous black shale (Mlakar and Drovenik 1971). A further possible source of sedimentary sulfur could be the Upper Ladinian beds, which contain sedimentary pyrite with $\delta^{34}S$ values between -7.8 and $+59.6‰$. This large spread of the $\delta^{34}S$ values points to bacterial activity in a system closed to SO_4^{2-}, and at least partially open to H_2S (e.g. Ilchik and Rumble 2000). This is in line with the paleoenvironmental reconstruction, according to which the Upper Ladinian beds with the highest $\delta^{34}S_{FeS2}$ values (kaolinite beds and conglomerate; Fig. 2) were deposited in a restricted, fresh water environment, with no or very limited connection to the sea (e.g. Placer and Čar 1977).

In summary, the large variation of the cinnabar $\delta^{34}S$ values at deposit down to hand-specimen scale is attributed to different mixing ratios between magmatic and other sulfur sources (seawater and evaporitic sulfates, pyrite, and organic sulfur).

Remobilization

A system of intersecting veinlets in the concordant Skonca orebodies, filled with cinnabar, native mercury, gangue minerals, and organic matter, is thought to have formed during multiphase remobilization throughout burial and the Alpine uplift (Mlakar and Drovenik 1971). Even though the conditions during remobilization are uncertain, they were very likely reducing due to the presence of organic matter-rich rocks. During remobilization, a part of the reduced sulfur in the system may have originated from reduction of ^{34}S-enriched pore-fluid sulfate. This would explain the more positive $\delta^{34}S$ values for cinnabar infilling the veinlets (median $= +14.7‰$), compared to cinnabar from the enclosing concordant orebodies (median $= +0.8‰$), in which a magmatic input is postulated. The same process could apply for cinnabar from veinlets (median $= +8.2‰$) that crosscut the Upper Ladinian conglomerates (median $= +4.2‰$). An alternative explanation for the observed $\delta^{34}S$ shift could be preferential loss of isotopically light sulfur during oxidation of cinnabar. The cinnabar-native mercury assemblage is frequently observed in active continental hot springs (e.g. Varekamp and Buseck 1984 and references therein), and was recently reported also from a submarine hydrothermal system (Bay of Plenty; Stoffers et al. 1999). As pointed out by Mlakar (1996), no secondary mercury minerals were observed to support oxidation as the source of native mercury. Additionally, the abundant organic matter in the host rocks could maintain reducing conditions, stabilizing native mercury. The large quantity of native mercury and the absence of significant alteration of the host rocks furthermore suggest limited post-Ladinian fluid circulation. Although oxidation processes were apparently not of major importance, a minor contribution of native mercury from oxidation of cinnabar cannot be excluded. The occurrence of isotopically heavy vein cinnabar ($+22.8‰$) associated with native mercury from a part of the mine that has been open for several 100s of years (level I), could be related to oxidation.

Ore deposition, role of organic matter and source of mercury

The physicochemical changes that can cause deposition of cinnabar and native mercury include decrease of pH and temperature, boiling, dilution and increase of fO_2 (e.g. Varekamp and Buseck 1984; Barnes and Seward 1997). Most of these mechanisms could have caused the deposition of the concordant orebodies. The reducing and low-pH swamp environment acted as a highly efficient geochemical trap for the precipitation of cinnabar and native mercury, reducing the quantity of mercury that could escape to the ecosystem.

The relative proportions of ore precipitated during mineralization phases I and II are not known. Only a little fraction of the mineralization can be undoubtedly attributed to mineralization phase I. Clearly associated with mineralization phase II are the orebodies in the Upper Ladinian lithologies and those controlled by the Middle Triassic unconformities. These orebodies represent the major portion of the high-grade orebodies that were mined in Idrija, i.e. mineralization phase II was quantitatively much more important than phase I. This is in agreement with the volcanic activity being strongest during uppermost Ladinian, as evidenced by the up to 80 m-thick layer of tuff that covered the deposit.

Conventionally, the major part of mercury transport in hydrothermal systems is thought to occur as Hg^0 in a gaseous phase or as Hg^0 and/or bisulfide complexes in an aqueous phase (e.g. Varekamp and Buseck 1984). Experimental studies have demonstrated that the solubility of mercury in short-chain normal alkanes (C_5 to C_{10}) is approximately two orders of magnitude greater than in the aqueous phase under the same physicochemical conditions (Fein and Williams-Jones 1997, and references therein). The close association of mercury mineralization and organic matter at Idrija suggests that

mercury may have been transported also in an organic phase. The Permocarboniferous shale and the Upper Permian dolostone were the source of hydrothermal petroleum, which formed by alteration and remobilization of indigenous organic matter (Lavrič and Spangenberg 2002). However, this does not imply that these rocks were the source of mercury. A trace element study of the regional geochemical background of the Idrija area found mercury concentrations considerably higher than the Clarke values for all investigated lithologies (average 0.7 ppm Hg for carbonates), with highest concentrations for the Upper Ladinian volcanic rocks and tuffs (up to 13 ppm Hg; Čadež et al. 1981). This finding agrees with the magmatic isotopic signature of the ore sulfides. Together with the geological and geochemical characteristics of the deposit, it confirms the genetic link between Ladinian volcanism and mineralization, but still does not provide a direct evidence for the source of mercury. The background mercury content of the Permocarboniferous shale was found to be less than 1 ppm (Čadež et al. 1981). The estimated initial total quantity of mercury in the Idrija deposit is between 250,000 and 300,000 t Hg (Placer 1982). The accumulation of such a quantity of mercury would require the extraction from $\sim$100 to 120 km^3 of shale with 1 ppm Hg. A much larger hydrothermal system with a volume of up to 300 km^3 would be required, if the Clarke value for shales is taken into account (0.4 ppm Hg; e.g. Barnes and Seward 1997). In the Idrija region there is no field evidence for a fossil hydrothermal system of that size. Considering all available geological and geochemical data a deep-seated source of mercury is most probable. A contribution of mercury from the Permocarboniferous black shale, which is likely to have contained the largest initial mercury concentration, cannot be excluded.

Isotopic variations of carbonates

The carbonates were depleted in ^{18}O and to a lesser extent in ^{13}C during mineralization. This isotopic shift is best observed in a profile in Upper Permian dolostone. The coupled ^{18}O (up to 3‰) and ^{13}C (up to 1‰) depletion in a highly fractured mineralized zone (Fig. 9) indicates isotopic re-equilibration of the host carbonates by circulating isotopically lighter fluids. The relatively steeper ^{18}O and ^{13}C gradients at the transition from less to more fractured host rocks, and the similar isotopic composition of the regional host carbonates and barren host carbonates from the mine record the highly channeled nature of the Idrija hydrothermal system.

To get further insight into the fluid source and nature of the fluid-rock interaction, the δ^{13}C and δ^{18}O variation ($r^2 = 0.57$; Fig. 10) of the Upper Permian dolostone was quantitatively modeled using a computer program (Spangenberg 1995) based on the mass balance equations from Zheng and Hoefs (1993). The modeling
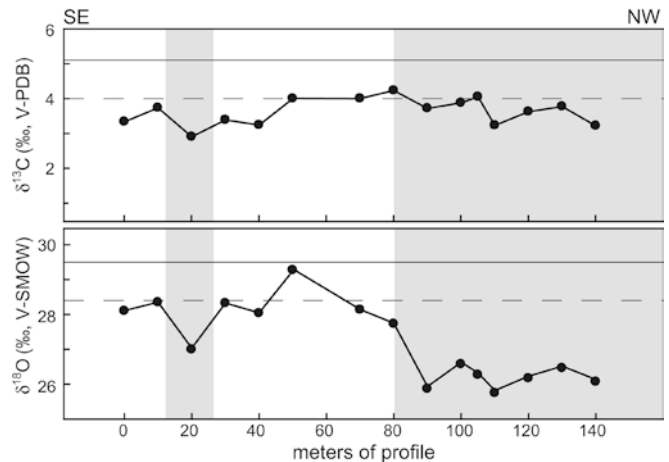

Fig. 9 Coupled δ^{13}C and δ^{18}O variation in a highly fractured mineralized zone, observed in a profile parallel to bedding in Upper Permian dolostone on level IV of the Idrija mine. The *white and gray areas* denote less and more fractured host rocks, respectively. The *solid and dashed lines* mark the median isotopic compositions of regional and mine samples of Upper Permian dolostone, respectively
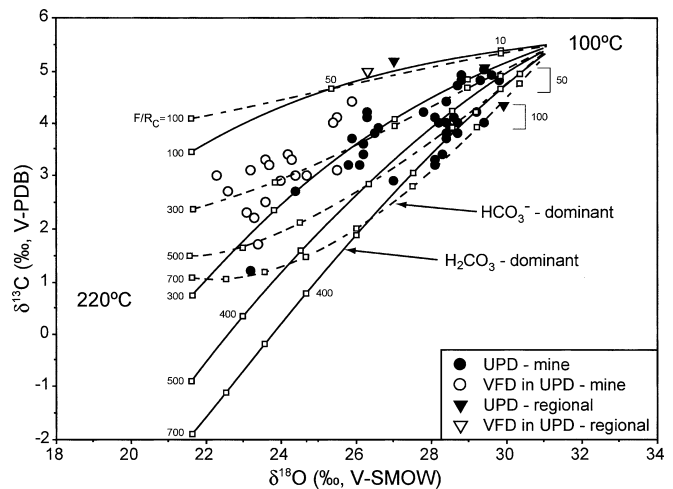

Fig. 10 δ^{13}C vs. δ^{18}O of the Upper Permian host dolostone (UPD) and associated void-filling dolomite (VFD). The calculated curves simulate dissolution of the host dolostone (H$_2$CO$_3$-dominant fluid with δ^{13}C$=-4$‰ and δ^{18}O$=+10$‰) and concomitant precipitation of the void-filling dolomite (HCO$_3^-$-dominant fluid with δ^{13}C$=-3$‰ and δ^{18}O$=+10$‰) at temperatures between 100 and 220 °C, and different cumulative fluid/rock weight ratios (F/R$_C$) marked with open squares (see text for details)

parameters took into account the variations of temperature, concentrations of dissolved carbon species (H$_2$CO$_3$, HCO$_3^-$), the initial isotopic composition of host carbonate and fluid, and the cumulative fluid-rock ratio. A deep-seated fluid is assumed to be slightly acidic, with the dissolved carbon in the form of H$_2$CO$_3$, with a δ^{13}C value of -4‰ and δ^{18}O value of $+10$‰ at a temperature of $\sim$220 °C. This temperature is consistent with the measured homogenization temperatures of fluid inclusions (160–218 °C; Palinkaš et al. 2001). The isotopic composition of this fluid is compatible with a deep-

seated fluid modified by isotopic exchange under low fluid/rock ratios with ^{18}O-rich minerals, particularly carbonates. The δ^{18}O value of the fluid was estimated from the oxygen isotopic composition of the void-filling dolomite, using the equation of Robinson and Ohmoto (1973) for isotopic equilibrium between water and dolomite. For temperatures between 160 and 220 °C the calculated δ^{18}O values of the fluid lie between $\sim+6$ and $\sim+15$‰. The precursor host carbonate is represented by regional, hydrothermally unaltered Upper Permian dolostone (δ^{13}C $\approx +5.5$‰ and δ^{18}O $\approx +29.4$‰), for which we assume 100 °C as the temperature of the pore fluid. This temperature approximately corresponds to burial of 0.5–1.0 km at an increased geothermal gradient (e.g. Polster and Barnes 1994), as it can be expected for the Idrija area in the Middle Triassic. The isotopic composition of the fluid depends on the modeled temperatures. Most data points are enclosed in the field limited by the calculated curves, which simulate precipitation of dolomite by fluid-rock interaction at temperatures between 100 and 220 °C, and different cumulative fluid/rock ratios (Fig. 10). The more inclined curves (solid lines in Fig. 10) simulate dissolution/recrystallization of the host carbonate by an incoming, slightly acidic mineralizing fluid (δ^{13}C ≈ -4‰ and δ^{18}O $\approx +10$‰, H_2CO_3 dominant). Dissolution of the host carbonate induced a change of the pH of the fluid, and a shift of the dominant dissolved carbon species from H_2CO_3 to HCO_3^-. The concave curves (dashed lines in Fig. 10) simulate the concomitant precipitation of dolomite from a fluid (δ^{13}C ≈ -3‰ and δ^{18}O $\approx +10$‰, HCO_3^- dominant), which evolved during exchange with the host carbonates. The coupled δ^{13}C and δ^{18}O changes of the host dolostone can be explained by carbonate dissolution/recrystallization from a H_2CO_3 dominant fluid during temperature increase (~100 to ~220 °C), combined with fluid/rock interaction (e.g. Spangenberg et al. 1996).

Conclusions

The stable isotope data of the ore and gangue minerals from the Idrija mercury deposit provide insights into the fluid source, the character and extent of the hydrothermal alteration, and the post-ore transformation of the mineralization.

The δ^{13}C and δ^{18}O values of the Idrija carbonates record a fracture-controlled hydrothermal system. The isotopic composition of the host and gangue carbonates matches quantitative models of temperature-dependent fluid-rock interaction in terms of dissolution of the host dolomite by a deep-seated hydrothermal fluid, and consequent precipitation of void-filling dolomites. The new isotopic data combined with paleoenvironmental reconstruction of previous investigators, suggest that the hydrothermal fluids at Idrija were a mixture of evolved fluids (seawater/meteoric water-derived) and magmatic fluids.

The stable isotopic signatures of sulfur minerals indicate disequilibrium conditions during ore deposition, and suggest that, in addition to the previously proposed magmatic and evaporitic sources, contemporaneous seawater sulfate, sedimentary pyrite and organic sulfur compounds contributed sulfur to the mineralization. Different mixing ratios between these sulfur sources, combined with long-term changes of the physicochemical conditions during the evolution of the Idrija hydrothermal system, are responsible for the large δ^{34}S variations of the ore sulfides at deposit down to hand-specimen scale. The shift toward more positive δ^{34}S values for the late cinnabar is attributed to a contribution of isotopically heavier pore-water sulfur during remobilization. A minor portion of the isotopically heavy cinnabar could represent the remnant of oxidation processes.

The large accumulation of mercury at Idrija cannot be explained solely by leaching of the Permocarboniferous shale. Deep faults of the Middle Triassic Idrija structure focused the regional-scale fluid flow and served as conduits for the transfer of mercury from greater depths. The abundant organic matter and the low-pH environment of the Upper Ladinian swamp were probably crucial for the formation of the high-grade ore at Idrija.

References

Aquilina L, Dia AN, Boulègue J, Bourgois J, Fouillac AM (1997) Massive barite deposits in the convergent margin off Peru: implications for fluid circulation within subduction zones. Geochim Cosmochim Acta 61:1233–1245

Barnes HL, Seward TM (1997) Geothermal systems and mercury deposits. In: Barnes HL (ed) Geochemistry of hydrothermal ore deposits, 3rd edn. Wiley, New York, pp 699–736

Berce B (1958) Geology of the Idrija mercury deposit (in Slovene with English summary). Geologija 4:5–62

Berce B (1965) The use of mercury in geochemical prospecting for mercury. Econ Geol 60:1516–1528

Boctor NZ, Shieh YN, Kullerud G (1987) Mercury ores from the New Idria Mining District, California: geochemical and stable isotope studies. Geochim Cosmochim Acta 51:1705–1715

Blumer M (1975) Curtisite, idrialite and pendletonite, polycyclic aromatic hydrocarbon minerals: their composition and origin. Chem Geol 16:245–256

Buser S (1987) Development of the Dinaric and the Julian carbonate platforms and of the intermediate Slovenian basin (NW Yugoslavia). Mem Soc Geol Ital 40:313–320

Čadež F (1977) Gypsum and anhydrite occurrences in Idria region (in Slovene with English abstract). Geologija 20:289–301

Čadež F, Hudnik V, Gogala A (1981) Trace elements in the Idrija ore deposit country rocks (in Slovene with English summary). Min Metall Q 28:33–43

Čar J (1975) Olisthostromes in the Idrija Middle Triassic trough-fault (in Slovene with English summary). Geologija 18:157–183

Čar J (1985) Development of the Middle Triassic sediments in the Idrija tectonic trough (in Slovene). PhD Thesis, University of Ljubljana, 236 pp

Čar J (1990) Angular tectonic-erosional unconformity in the deposit's part of the Idrija Middle Triassic tectonic structure (in Slovene with English summary). Geologija 31–32:267–284

Chiba H, Sakai H (1985) Oxygen isotope exchange rate between dissolved sulphate and water at hydrothermal temperatures. Geochim Cosmochim Acta 49:993–1000

Claypool GE, Holser WT, Kaplan IR, Sakai H, Zak I (1980) The age curves of sulfur and oxygen isotopes in marine sulfate and their mutual interpretation. Chem Geol 28:199–260

Drovenik M, Čar J, Strmole D (1975) Langobard-Tongesteine in der Idrija Lagerstätte (in Slovene with German summary). Geologija 18:107–155

Drovenik M, Duhovnik J, Pezdič J (1976) The sulfur isotope composition of sulfides from ore deposits in Slovenia (in Slovene with English summary). Min Metall Q 24:193–246

Drovenik M, Pleničar M, Drovenik F (1980) The origin of Slovenian ore deposits (in Slovene with English summary). Geologija 23:1–157

Drovenik M, Dolenec T, Režun B, Pezdič J (1991) On the mercury ore from the Grübler orebody, Idrija (in Slovene with English summary). Geologija 33:397–446

Fein JB, Williams-Jones AE (1997) The role of mercury-organic interactions in the hydrothermal transport of mercury. Econ Geol 92:20–28

Friedman I, O'Neil JR (1977) Compilation of stable isotope fractionation factors of geochemical interest. In: Fleischer M (ed) Data of geochemistry. Ch KK US Geol Surv Prof Pap 440-KK, pp 1–12

Giesemann A, Jager HJ, Norman AL, Krouse HP, Brand WA (1994) Online sulfur-isotope determination using an elemental analyzer coupled to a mass-spectrometer. Anal Chem 66 (18):2816–2819

Herzig PM, Hannington MD, Arribas Jr A (1998) Sulfur isotopic composition of hydrothermal precipitates from the Lau backarc: implications for magmatic contributions to seafloor hydrothermal systems. Miner Deposita 33:226–237

Ilchik RP, Rumble D (2000) Sulfur, carbon, and oxygen isotope geochemistry of pyrite and calcite from veins and sediments sampled by borehole CCM-2, Creede caldera, Colorado. Geol Soc Am Spec Pap 346:287–300

Krouse RH, Viau CA, Eliuk LS, Ueda A, Halas S (1988) Chemical and isotopic evidence of thermochemical sulfate reduction by light hydrocarbon gases in deep carbonate reservoirs. Nature 333:415–419

Kusakabe M, Mayeda S, Nakamura E (1990) S, O and Sr isotope systematics of active vent materials from the Mariana backarc basin spreading axis at 18°N. Earth Planet Sci Lett 100:275–282

Lavrič JV, Spangenberg JE (2001) Geochemistry of the Idrija mercury deposit, Slovenia: insights from $\delta^{13}C$, $\delta^{18}O$, $\delta^{34}S$ and organic geochemical data. In: Piestrzyński et al (eds) Mineral deposits at the beginning of the 21st century, Swets & Zeitlinger, Lisse, pp 55–58

Lavrič JV, Spangenberg JE (2002) Aromatic hydrothermal petroleum from a mercury deposit (Idrija, Slovenia). V. M. Goldschmidt Conference 2002, 18–23 August, 2002, Davos, Switzerland. Geochim Cosmochim Acta 66, S1:A435

Leśniak PM, Łącka B, Hladíkova J, Zieliński G (1999) Origin of barite concretions in the West Carpathian flysch, Poland. Chem Geol 158:155–163

McCrea JM (1950) On the isotopic chemistry of carbonates and a paleotemperature scale. J Chem Phys 18:849–857

Mlakar I (1967) Relations between the lower and the upper structure of the Idrija ore deposit (in Slovene with English summary). Geologija 10:87–126

Mlakar I (1969) Nappe structure of the Idrija-Žiri region (in Slovene with English summary). Geologija 12:5–72

Mlakar I, Drovenik M (1971) Structural and genetic particularities of the Idrija mercury ore deposit (in Slovene with English summary). Geologija 14:67–126

Mlakar I (1974) An outline of production of the Idrija mercury mine through centuries (in Slovene with English summary). Idrijski Razgledi 3–4, XIX:1–40

Mlakar I (1996) On the Marija Reka mercury deposit and its comparison with the Litija and Idrija deposits from the aspect of plate tectonics (in Slovene with English summary). Geologija 37–38:321–376

Ohmoto H, Goldhaber MB (1997) Sulfur and carbon isotopes. In: Barnes HL (ed) Geochemistry of hydrothermal ore deposits, 3rd edn. Wiley, New York, pp 517–611

Ozerova NA, Vinogradov VI, Mlakar I, Fedorchuk VP, Titov IN (1973) Isotopic composition of the sulfur of some ores from ore deposits in the western part of the Mediterranean mercury belt (in Russian). In: Shipulin FK, Feodotiev KM (eds) Abstract of the geochemistry of selected elements, Izdat Nauka, Moscow, pp 275–310

Palinkaš LA, Strmić S, Herlec U (2001) The ore-forming fluids in the Idria mercury mine, Slovenia. In: Piestrzyński et al. (eds) Mineral deposits at the beginning of the 21st century, Swets & Zeitlinger, Lisse, pp 321–324

Peabody CE, Einaudi MT (1992) Origin of petroleum and mercury in the Culver-Baer cinnabar deposit, Mayacmas district, California. Econ Geol 87:1078–1103

Placer L (1973) Reconstruction of the nappe structure of the Idrija-Žiri region (in Slovene). Geologija 16:317–334

Placer L (1975) The texture analysis of the epigenetic Gruebler ore body in the Idrija ore deposit (in Slovene with English summary). Min Metall Q 23:3–28

Placer L (1976) Structural control of the epigenetic ore bodies of the Idria ore deposit (in Slovene with English summary). Min Metall Q 24:3–30

Placer L (1982) Structural history of the Idrija mercury deposit (in Slovene). Geologija 25:7–94

Placer L, Čar J (1977) The Middle Triassic structure of the Idrija region (in Slovene with English summary). Geologija 20:141–166

Polster W, Barnes HL (1994) Comparative hydrodynamic and thermal characteristics of sedimentary basins and geothermal systems in sediment-filled rift valleys. In: Ortoleva PJ (ed) Basin compartments and seals. Am Assoc Petrol Geol Mem 61: 437–457

Robinson BW, Ohmoto H (1973) Mineralogy, fluid inclusions, and stable isotopes of the Echo Bay U-Ni-Ag-Cu deposits, Northwest Territories, Canada. Econ Geol 68:635–656

Rosenbaum J, Sheppard SMF (1986) An isotopic study of siderites, dolomites and ankerites at high temperatures. Geochim Cosmochim Acta 50:1147–1150

Rye RO, Plumlee GS, Bethke PM, Barton PB (1988) Stable isotope geochemistry of the Creede, Colorado hydrothermal system. US Geol Surv Open-File Rep 88–356: 41 pp

Spangenberg JE (1995) Geochemical (elemental and isotopic) constraints on the genesis of the Mississippi Valley-type zinc-lead deposit of San Vicente, central Peru. Terre Environ 1:123 pp

Spangenberg JE, Fontboté L, Sharp ZD, Hunziker J (1996) Carbon and oxygen isotope study of hydrothermal carbonates in the zinc-lead deposits of the San Vicente district, central Peru: a quantitative modeling on mixing processes and CO_2 degassing. Chem Geol 133:289–315

Spangenberg JE, Hunziker J, Meisser N, Herlec U (1999) Compound specific isotope analysis of the organic minerals hatchettite and idrialite in geodes, coal, and mineral deposits. In: Stanley CJ et al. (eds), Mineral deposits: processes to processing. Balkema, Rotterdam, pp 275–278

Stoffers P, Hannington M, Wright I, Herzig P, deRonde C (1999) Elemental mercury at submarine hydrothermal vents in the Bay of Plenty, Taupo volcanic zone, New Zealand. Geology 27: 931–934

Strunz H, Contag B (1965) Evenkit, Flagstaffit, Idrialin und Reficit. Neues Jahrb Miner Monatsh 1:19–25

Varekamp JC, Buseck PR (1984) The speciation of mercury in hydrothermal systems, with applications to ore deposition. Geochim Cosmochim Acta 48:177–185

White DE (1981) Active geothermal systems and hydrothermal ore deposits. Econ Geol 75th Aniv Vol, pp 392–423

Wise JA, Campbell RM, West WR, Lee ML, and Bartle KD (1986) Characterization of polycyclic aromatic hydrocarbon minerals curtisite, idrialite, and pendeltonite using high-performance liquid chromatography, gas chromatography, mass spectrometry and nuclear resonance spectroscopy. Chem Geol 54:339–357

Zheng YF, Hoefs J (1993) Carbon and oxygen isotopic covariations in hydrothermal calcites—theoretical modeling on mixing processes and application to Pb-Zn deposits in the Harz Mountains, Germany. Miner Deposita 28:79–89